USRP Implementation of Transmission Timing Control Function for Synchronized SS-CDMA Using Wireless Two-Way Interferometry (Wi-Wi)

Suguru Kameda[†,¶], Yusaku Honma[†,‡], Noriharu Suematsu[†], Satoshi Yasuda[§], Nobuyasu Shiga[§]
[†] Research Institute of Electrical Communication, Tohoku University
2–1–1 Katahira, Aoba-ku, Sendai 980–8577, Japan
[‡] Graduate School of Engineering, Tohoku University
[§] National Institute of Information and Communications Technology (NICT)
4–2–1 Nukui-Kitamachi, Koganei, Tokyo 184–8795, Japan
[¶] Research Institute for Nanodevice and Bio Systems, Hiroshima University
1–4–2 Kagamiyama, Higashi-Hiroshima 739–8527, Japan
Email: kameda3@hiroshima-u.ac.jp

***Abstract*—Synchronized spread spectrum code division multiple access (SS-CDMA) is very effective for increasing the capacity and reducing the interference with a rapid spread of Internet of things (IoT) devices. Since the synchronized SS-CDMA requires to receive timing synchronization, it is essential to realize transmission timing control of each node using space-time synchronization. In this paper, we investigate precise time synchronization between nodes using Wireless Two-Way Interferometry (Wi-Wi). The measurement results show that the precision of initial timing synchronization of the Wi-Wi module is nearly equal to 400 ns. Furthermore, we implement transmission timing control function on Universal Software Radio Peripheral (USRP) synchronized by reference signals of Wi-Wi module. As a result of the measurement evaluation of the implemented system, it is realized that the transmission timing is controlled at the accuracy of the sampling rate of USRP.**

***Index Terms*—synchronized SS-CDMA, transmission timing control, time synchronization, software defined radio**

I. Introduction

In recent years, the Internet of things (IoT) devices have been spreading rapidly, and further growth is expected in the future. In particular, industrial applications are expected to grow remarkably due to the expansion of smart factories and smart cities. As a result, the increase of autonomous transmissions by nodes and the increase of radio interference due to the expansion of frequency sharing will become a serious problem, especially in the uplink where information is sent from each node to the network.

Synchronized spread spectrum code division multiple access (synchronized SS-CDMA) [1]–[3] is a highly efficient communication method to solve these problems. Fig. 1 shows a conceptual diagram of synchronized SS-CDMA using space-time synchronization. We consider that multiple nodes transmit signals to an access point (AP) at the same time using the same frequency. In the synchronized SS-CDMA, the local clock of each node is synchronized with those of AP by using reference signals. Each node calculates the precise distance between the AP and its own location, and estimates the propagation delay using the distance. All nodes transmit their modulated signals at a suitable time so that all signals arrive at the AP at the same time.

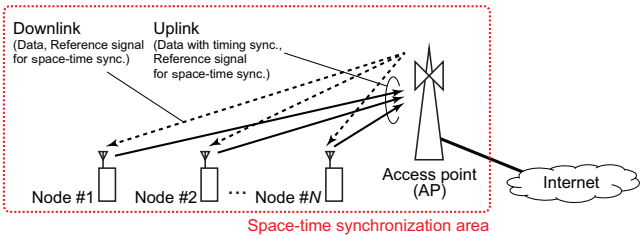

Fig. 1. Conceptual diagram of synchronized SS-CDMA with space-time synchronization.

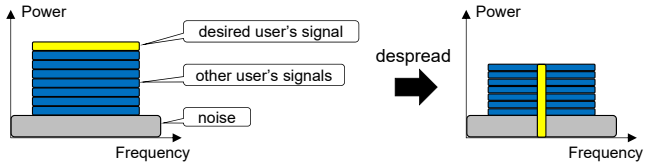

(a) Typical asynchronous CDMA

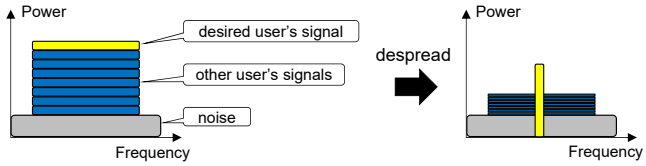

(b) Synchronized SS-CDMA

Fig. 2. Spectrum of received uplink signals before and after despreading.

Fig. 2 shows the spectrum of received uplink signals before and after despreading. Fig. 2(a) shows the spectrum of a typical uplink asynchronous CDMA. The horizontal axis shows the frequency. The vertical axis shows the power. The figures

left- and right-hand sides of the black arrow indicate the spectrums before and after despreading, respectively. Before despreading, the desired node signal and interfering node signals are spread over a wide band. After despreading, although the desired node signal is despread to the original signal, the desired node signal cannot be demodulated. The desired node signal is buried in the interfering node signals since there is no orthogonality between the asynchronous uplink signals. Fig. 2(b) shows the spectrum of uplink synchronized SS-CDMA. In the synchronized SS-CDMA with synchronization of reception timing between the uplink signals, orthogonal codes such as orthogonal M-sequence is used as spreading codes. The orthogonal code here refers to the code whose cross-correlation value is zero at zero phase shift. The interfering node signals can be suppressed after the despreading because of orthogonality realized by using orthogonal code with timing synchronization. Therefore, synchronization of receiving timing is essential for realizing the synchronized SS-CDMA.

In order to achieve reception timing synchronization in the uplink, it is necessary to control the transmission timing of signals sent from each node. For controlling the timing of transmission, it is necessary to achieve space-time synchronization, i.e., a state in which multiple distant nodes are synchronized by sharing a single clock and each node knows the other's location. By grasping each other's location, each node can control the transmission timing according to the distance to the AP. This enables synchronization of the reception timing between uplink signals. In our previous works [1]–[3], we have proposed to use Quasi-Zenith Satellite System (QZSS) and Global Positioning System (GPS) positioning signals for space-time synchronization. However, the application of satellite positioning systems is difficult when considering indoor applications such as smart factories.

Wireless Two-Way Interferometry (Wi-Wi) has been proposed as a technique to achieve local space-time synchronization even indoors [4], [5]. It achieves highly accurate space-time synchronization using only wireless two-way communication between distant nodes, and is applicable to indoor environments. Hereinafter, the terminal implementing this technology is called Wi-Wi module.

In this paper, we implement and evaluate the transmission timing control function of synchronized SS-CDMA using Wi-Wi module and Universal Software Radio Peripheral (USRP). Note that in this paper for a feasibility investigation, only the time synchronization function is implemented and evaluated. In Sect. II, the Wi-Wi technology is described simply. In Sect. III, we will evaluate the initial time synchronization accuracy of the Wi-Wi module, called timing offset in this paper, by measuring and comparing the 1-pps signals output by the two time-synchronized Wi-Wi modules. In Sect. IV, we will implement and evaluate the method of synchronizing to the external reference signal of USRP and the transmission timing control method. Finally, in Sect. V, we will conclude this paper.

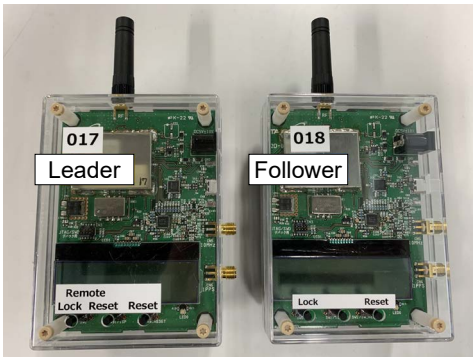

Fig. 3. Photograph of Wi-Wi module.

II. Overview of Wi-Wi

In this section, we briefly explain Wi-Wi, a wireless two-way time comparison technology [4], [5]. The Wi-Wi module used in this implementation is shown in Fig. 3. The left one is the leader module and the right one is the follower module. They communicate with each other using the antenna on the top of the module in the 925-MHz band. Eight time slots are prepared in advance, and up to seven follower modules can communicate with one leader module in a time-shared manner. The two ports on the right side output 10-MHz and 1-pps signals, respectively.

It has already been demonstrated that Wi-Wi can be used to measure clock variations with high accuracy of ps order [4]. This was made possible by applying carrier-phase two-way satellite frequency transfer (TWCP) [6], which uses carrier phase for time and frequency comparison between two nodes. Therefore, by using the 10-MHz signal output by the synchronized Wi-Wi module as the clock reference signal, the clock between the two USRP terminals can be synchronized with high accuracy of ps order. In the same way, it has already been demonstrated that mm-order accuracy distance variation measurement is possible by using Wi-Wi [5].

III. Evaluation of Timing Offset of 1-pps Output from Wi-Wi Module

In Sect. II, it was described that the 10-MHz signal output by the Wi-Wi module can be used to synchronize the clock with high accuracy of ps order. It can be realized to keep the time synchronization of the 1-pps signal output by the Wi-Wi module with high accuracy. However, the accuracy of the timing offset of the 1-pps signal has not been evaluated yet. In particular, in a real environment, the timing offset of the 1-pps signal may be degraded due to degradation factors such as multipath. Therefore, in this section, we measure the timing offset of the 1-pps signal output from the Wi-Wi module, which is synchronized between two modules, in several different environments.

Fig. 4 shows the photograph of measurement system in the anechoic chamber. Fig. 4(a) shows the measurement system in the case of a wired connection between the leader and follower of the Wi-Wi modules. The leader and follower of the Wi-Wi

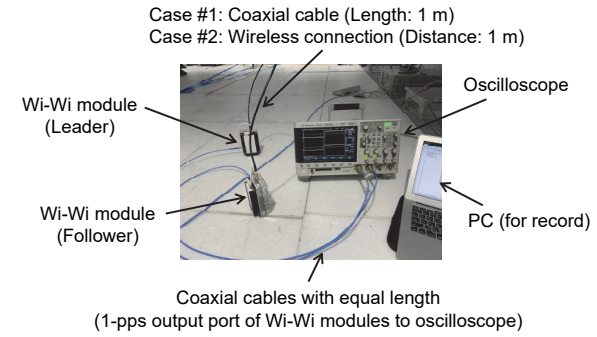

(a) Measurement system

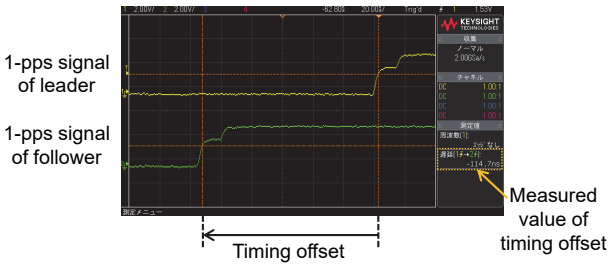

(b) Example of the oscilloscope screen

Fig. 4. Photograph of measurement system in the anechoic chamber.

(a) panoramic view of the corridor

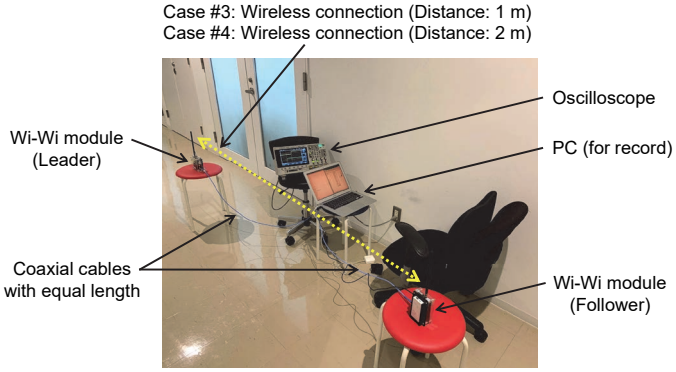

(b) Measurement system

Fig. 5. Photograph of measurement system in the corridor.

module were made to communicate with each other, and the output 1-pps signals were input to channels 1 and 2 of an oscilloscope, Keysight DSO-X 3034A, respectively. The 1-pps signal output port and the oscilloscope were connected with an equal length cable of 1.5 m. Fig. 4(b) shows an example of the oscilloscope screen. The yellow waveform at the top is the output signal of the leader. The green waveform at the bottom is the output signal of the follower. The values surrounded by the orange dashed frame are the measured values of the timing offset. In this measurement, we recorded the measured values displayed on the screen of the oscilloscope.

The Wi-Wi module starts communication for synchronization with pressing the "Lock" button in Fig. 3 and locks the 1-pps signal in a time-synchronized state by comparing each other's time for a few seconds. After that, the time synchronization is maintained until the "Reset" button is pressed. In this evaluation, we repeatedly reset and lock the Wi-Wi module, and record the timing offset immediately after locking to create a histogram. The histograms are then compared under different conditions, such as different signal environments and different distances between modules.

A. Measurement under varying radio-wave environments

We conducted measurements in the following three different environments. Case #1 is a wired connection with a coaxial cable of 1 m. Case #2 is a wireless connection in an anechoic chamber with a distance of 1 m between the leader and follower. Case #3 is a wireless connection at a distance of 1 m in a corridor with line-of-sight (LOS) condition. Fig. 5(a) shows the photograph of the panoramic view of the corridor. There are metal boards on a wall of the corridor. The measurements were performed at the location shown in the frame area of yellow broken line. Fig. 5(b) shows the measurement system in the case #3. This is the same as Fig. 4(a) except that the leader and follower of Wi-Wi modules are connected to each other wirelessly. In both cases, the modules were not moved during the measurements and there was no change in the surrounding radio environment.

Figs. 6(a), 6(b), and 6(c) show the measurement result of cases #1, #2, and #3, respectively. The number of trials in cases #1, #2, and #3 was set to 150, 100, and 200, respectively, as the number of times that the histogram takes the shape of a roughly normal distribution. When the initial synchronization time of the follower lags behind the initial synchronization time of the leader by α ns, the measured value of timing offset is recorded as $+\alpha$ ns. The class width is 50 ns.

There was no significant difference in the trend of the distribution depending on the radio environment. This is probably because there is no change in the radio environment within the measurement time in any of the environments, including case #3 where multipath exists. In all environments, the 3σ was around 400 ns. In both environments, the center of the distribution is negative. This may be due to the implementation problem of the initial time synchronization function of the Wi-Wi module.

B. Measurement with varying distance

Next, we measured by changing the distance between the leader and follower of the Wi-Wi module. As in case #3, the measurement was performed in the corridor shown in Fig. 5,

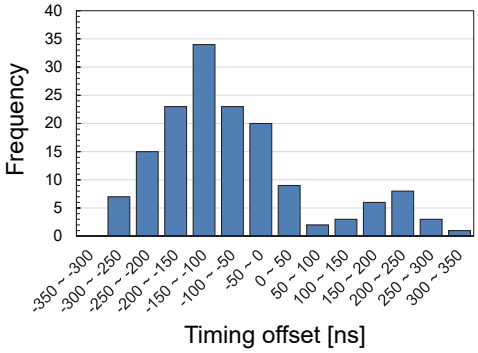

(a) Case #1: Wired connection

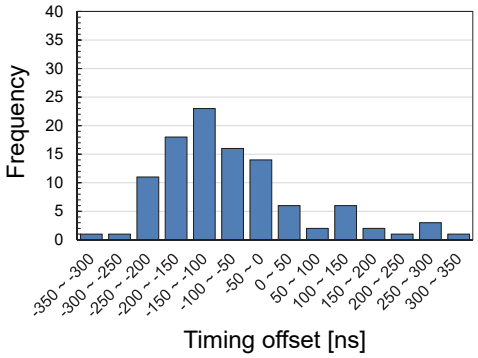

(b) Case #2: Anechoic chamber

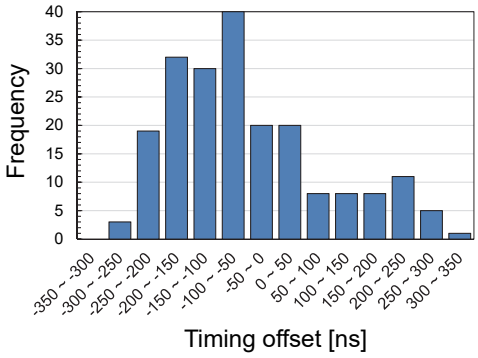

(c) Case #3: Corridor with LOS condition (Distance: 1 m)

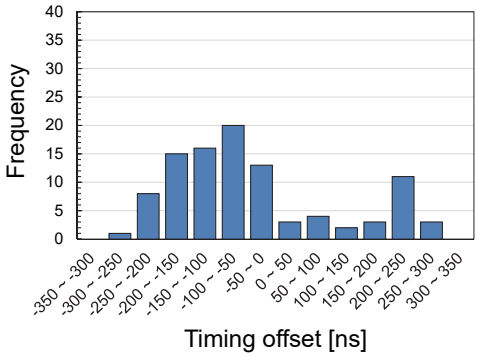

(d) Case #4: Corridor with LOS condition (Distance: 2 m)

Fig. 6. Evaluation of timing offset.

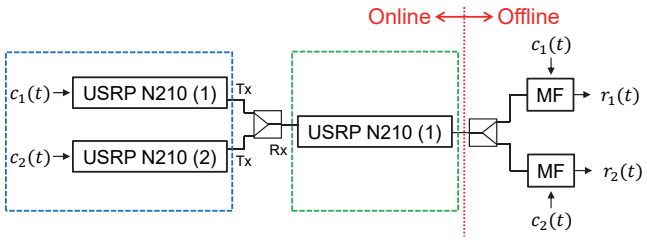

(a) Block diagram

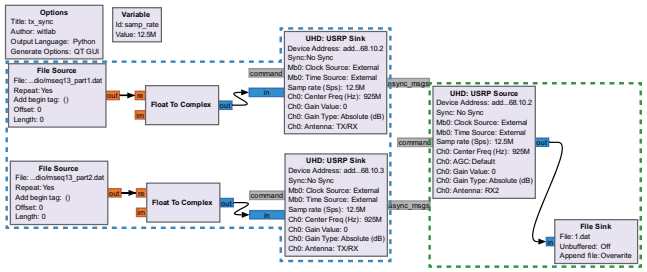

(b) Flow graph on GRC

Fig. 7. Implemented system of transmission timing control function.

and the distance between the modules was set to 2 m (case #4).

Fig. 6(d) shows the measurement result of the case #4. The number of trials was set to 100. Compared to case #3 in Fig. 6(c), there was no significant difference in the trend of the distribution. These results show that there is no significant change in the synchronization performance up to a communication distance of 2 m.

IV. Implementation and Evaluation of Transmission Timing Control Function for Synchronized SS-CDMA Using USRP

In this section, we implement and evaluate a function to control the transmission timing by synchronizing with an external reference signal in USRP. We use the output signal of the Wi-Wi module evaluated in Sect. III as the external reference signal for USRP.

A. Implementation of transmission timing control function

The block diagram of implemented system of transmission timing control function is shown in Fig. 7(a). Two USRP N210s with both transmission and reception functions were used. Transmission signals $c_1(t)$ and $c_2(t)$, which were created in MATLAB, were transmitted from the transmission part of USRP (1) and (2), respectively. The transmission signals were received by the reception part of USRP (1) after being combined by the combiner. The received signals were processed offline using MATLAB. The despreading process was performed using matched filter (MF) for $c_1(t)$ and $c_2(t)$ respectively.

We will explain in detail the real-time system (online part, left side of the red dashed line) in Fig. 7(a). USRP is controlled by GNU Radio on a personal computer (PC) connected via an Ethernet cable. Fig. 7(b) is the flow graph which is created

Listing 1
ADDITIONAL CODE USED IN THIS IMPLEMENTATION

```
1  self.uhd_usrp_source_0.set_time_next_pps(uhd.time_spec())
2  self.uhd_usrp_source_1.set_time_next_pps(uhd.time_spec())
3  self.uhd_usrp_sink_0.set_time_next_pps(uhd.time_spec())
4  time.sleep(1)
5  time_now = self.uhd_usrp_source_0.get_time_now() + uhd.time_spec(0.01)
6  self.uhd_usrp_source_0.set_command_time(time_now)
7  self.uhd_usrp_source_0.set_center_freq(925e6)
8  self.uhd_usrp_source_0.clear_command_time()
9  self.uhd_usrp_source_1.set_command_time(time_now)
10 self.uhd_usrp_source_1.set_center_freq(925e6)
11 self.uhd_usrp_source_1.clear_command_time()
12 self.uhd_usrp_sink_0.set_command_time(time_now)
13 self.uhd_usrp_sink_0.set_center_freq(925e6)
14 self.uhd_usrp_sink_0.clear_command_time()
15 while self.uhd_usrp_source_0.get_sensor("lo_locked").to_bool() != True:
16   pass
17 while self.uhd_usrp_source_1.get_sensor("lo_locked").to_bool() != True:
18   pass
19 while self.uhd_usrp_sink_0.get_sensor("lo_locked").to_bool() != True:
20   pass
21 time_now = self.uhd_usrp_source_0.get_time_now() + uhd.time_spec(0.1)
22 self.uhd_usrp_source_0.set_start_time(time_now)
23 self.uhd_usrp_source_1.set_start_time(time_now)
24 self.uhd_usrp_sink_0.set_start_time(time_now)
```

on the graphical tool GNU Radio Companion (GRC) on the PC. The parts surrounded by blue and green dashed lines correspond to the respective parts in Fig. 7(a).

Next, it is explained of implementation a function to synchronize the USRP time with the external 1-pps signal and control the timing of transmission. Since these functions cannot be implemented only using functions in GRC, it is necessary to generate Python code from GRC and to add specific code. In this implementation, we used an additional code to control the transmission timing of the two USRPs as described in Ref. [7]. The additional code used in this implementation is shown in Listing 1. This code was added before `#connections` in the code generated by GRC.

The details of the code in Listing 1 are described below. In lines 1 to 3, the two transmitters and one receiver of the USRP obtain the reference time from the 1-pps signals, respectively. In line 4, since it takes a maximum of one second to set the time after issuing the `set_time_next_pps()` command, `time.sleep(1)` is added. In lines 5 to 14, it is set the center frequency to a fixed simultaneously. In lines 15 to 20, it is waited until the local oscillator (LO) is locked. This fixes the phase of the LO. In lines 21 to 24, the start of USRP operation is set simultaneously to synchronize the timing of transmission and reception.

B. Evaluation of the implemented transmission timing control function

In this section, we evaluate the transmission timing control function implemented on USRPs connected with Wi-Wi modules described in Sect. IV-A. The block diagram and photograph of the measurement system are shown in Figs. 8(a) and 8(b), respectively. The 1-pps signal of output of each Wi-Wi module was branched by the power divider. One of them was input to the USRP and the other one to the oscilloscope to measure the timing offset of the 1-pps signal output from the Wi-Wi module. The signals output from the transmitters of USRP (1) and (2) were combined by combiners and then input to the receiver of USRP (1). Two USRPs were controlled by an Ubuntu PC via Ethernet cables and a switching hub. The sampling rate of the USRP was set to 12.5 MHz.

The transmitted signals $c_1(t)$ and $c_2(t)$ were different 13th-order M-sequences repeated for 12 periods. The generator polynomials of $c_1(t)$ and $c_2(t)$ were (1, 3, 4, 13) and (4, 5, 7, 8, 9, 10, 13), respectively. The carrier frequency and chip rate of the transmitted signals were set to 925 MHz and 12.5 Mchip/s, respectively. Each matched filter corresponded to a respective M-sequence used for the transmission signal. When the received signal was despread on the two matched filters, output signals $r_1(t)$ and $r_2(t)$ shown in Fig. 7(a) showed correlation peaks every 8,192 chip, which was the period of the 13th-order M-sequence. We evaluated the synchronization performance by comparing the time of the first of these correlation peaks. If the clock times of USRPs (1) and (2) are exactly the same and the transmit timing control function is working ideally, there will be no difference in the times of correlation peak of despread signals $r_1(t)$ and $r_2(t)$. If there is timing offset in the 1-pps signal output from the Wi-Wi module, there should be a time difference of correlation peak between $r_1(t)$ and $r_2(t)$. Therefore, as in Sect. III, we measured and evaluated the timing offset of the 1-pps signal outputs from the Wi-Wi modules and the time difference of the two correlation peaks that were despread by each matched filter.

Table I shows the measurement results of the implemented transmission timing control function. In this evaluation, 15 trials were conducted. The first column shows the trial number.

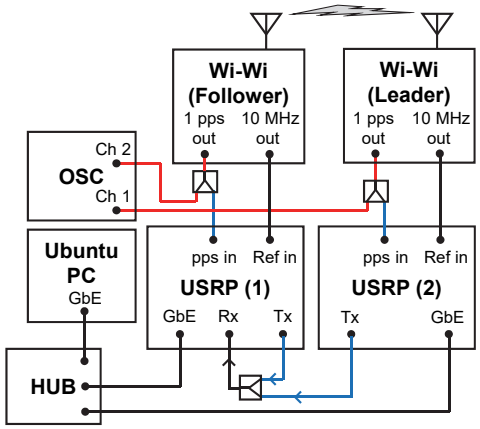

(a) Block diagram

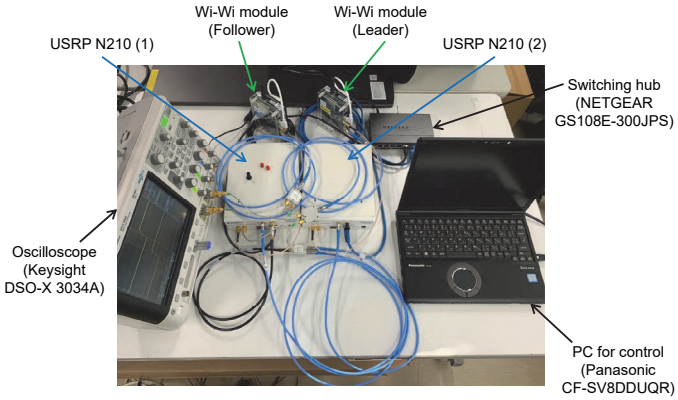

(b) Photograph

Fig. 8. Measurement system.

The second column (W) shows the timing offset of the 1-pps signals output by the Wi-Wi modules. The third column (U) shows the time difference of the correlation peaks of the signals that were despread by each matched filter. The fourth column (D) shows the difference between the values in the second and third columns, $D = W - U$. The results of 15 trials show that they were all $-40 < D < 40$. Since the sampling rate of the USRP was 12.5 MHz, which was the same as the chip rate of the transmitted signal, the accuracy of the time difference in the measurement system was ± 40 ns. Therefore, it means that the USRP was synchronized with the reference signal from the Wi-Wi module and the transmission timing was controlled at the accuracy of sampling rate of USRP.

V. Conclusions

In this paper, we implemented and evaluated the transmission timing control function of synchronized spread spectrum code division multiple access (SS-CDMA) using Wireless Two-Way Interferometry (Wi-Wi) module and Universal Software Radio Peripheral (USRP). At first, we investigated the precision of initial time synchronization of the Wi-Wi module. The measurement results show that the precision of initial timing synchronization of the Wi-Wi module (3σ) was nearly equal to 400 ns in the case of wireless connection with distance of 2 m. Next, we implemented transmission timing control function on USRP synchronized by reference signals of Wi-Wi module. As a result of the measurement evaluation of the implemented system, it was realized that the transmission timing was controlled at the accuracy of the sampling rate of USRP.

TABLE I
Meaturement results of the implemented transmission timing control function

Trial #	Wi-Wi W [ns]	USRP U [ns]	$D = W - U$ [ns]
1	206	240	−34
2	98	80	18
3	−193	−160	−33
4	137	160	−23
5	39	0	39
6	84	80	4
7	94	80	14
8	180	160	20
9	97	80	17
10	242	240	2
11	−99	−80	−19
12	111	80	31
13	58	80	−22
14	163	160	3
15	−189	−160	−29

Acknowledgment

This paper is based on results obtained from projects, JPNP20017, commissioned by the New Energy and Industrial Technology Development Organization (NEDO), and the Cooperative Research Project of the Research Institute of Electrical Communication, Tohoku University. The authors would like to thank Prof. Yoji Yamada and Mr. Tomoya Nakahama of National Institute of Technology, Ishikawa College, for their kindly advice regarding USRP implementation.

References

[1] S. Kameda, K. Ohya, R. Shinozaki, H. Oguma, and N. Suematsu, "Experimental evaluation of synchronization accuracy considering sky view factor for QZSS short message synchronized SS-CDMA," IEICE ComEX, vol. 7, no. 9, pp. 322–327, Sep. 2018.

[2] S. Kameda, A. Taira, Y. Miyake, N. Suematsu, T. Takagi, and K. Tsubouchi, "Evaluation of synchronized SS-CDMA for QZSS safety confirmation system," IEEE Trans. Veh. Tech., vol. 68, no. 5, pp. 4846–4856, May 2019.

[3] S. Kameda, K. Ohya, H. Oguma, and N. Suematsu, "Experimental evaluation of synchronized SS-CDMA transmission timing control method for QZSS short message communication," IEICE Trans. Commun., vol. E102–B, no. 8, pp. 1781–1790, Aug. 2019.

[4] N. Shiga, K. Kido, S. Yasuda, B. Panta, Y. Hanado, S. Kawamura, H. Hanado, K. Takizawa, and M. Inoue, "Demonstration of wireless two-way interferometry (Wi-Wi)," IEICE ComEX, vol. 6, no. 2, pp. 77–82, Feb. 2017.

[5] S. Yasuda, R. Ichikawa, Y. Hanado, S. Kawamura, H. Hanado, H. Iwai, K. Namba, Y. Okamoto, K. Fukunaga, T. Iguchi, and N. Shiga, "Horizontal atmospheric delay measurement using wireless two-way interferometry (Wi-Wi)," Radio Sci., vol. 54, no. 7, pp. 572–579, Jul. 2019.

[6] M. Fujieda, T. Gotoh, F. Nakagawa, R. Tabuchi, M. Aida, and J. Amagai, "Carrier-phase-based two-way satellite time and frequency transfer," IEEE Trans. Ultrason. Ferroelectr. Freq. Control, vol. 59, no. 12, pp. 2625–2630, Dec. 2012.

[7] T. Nakahama, Y. Yamada, and S. Kameda, "Example GNU radio implementations of phase alignment between USRP devices," IEICE Tech. Rep., vol. 120, no. 238, SR2020-34, pp. 74–81, Nov. 2020.